LOW-TEMPERATURE HYDROTHERMAL ALTERATION OF SILICIC GLASS AT THE PACMANUS HYDROTHERMAL VENT FIELD, MANUS BASIN: AN XRD, SEM AND AEM-TEM STUDY

Giovanna Giorgetti[1], Thomas Monecke[2], Reinhard Kleeberg[3] and Mark D. Hannington[2]

[1] Dipartimento di Scienze della Terra, Università di Siena, Via Laterina 8; 53100 Siena, Italy
[2] Department of Earth Sciences, University of Ottawa, Marion Hall, 140 Louis Pasteur, Ottawa, ON, K1N 6N5, Canada
[3] Institut für Mineralogie, TU Bergakademie Freiberg, Brennhausgasse 14, D-09596 Freiberg, Germany

Abstract—Dacitic lava recovered from the immediate subsurface of the submarine PACMANUS hydrothermal vent field exhibits variable degrees of hydrothermal alteration resulting from the interaction of the glassy volcanic rocks with mineralizing hydrothermal fluids at relatively low temperatures. Transmission electron microscopic (TEM) investigations revealed that the felsic volcanic glass transformed to nm-thick smectitic flakes of the montmorillonite-beidellite series *via* a dissolution and reprecipitation mechanism. The process of smectite formation did not proceed through X-ray amorphous or poorly crystalline transitional phases. Alteration of the glass was found to be most pronounced adjacent to perlitic cracks and vesicles that form an interconnected network focusing fluid flow. Glass dissolution adjacent to these fluid pathways resulted in a characteristic alteration texture at the nm scale; the intensely altered groundmass contains round cavities that are partially coated or filled by smectitic flakes. The Mg content of the smectite broadly increases towards the fluid pathways. Smectitic flakes with compositions corresponding to saponite occur in the intensely altered groundmass adjacent to perlitic cracks. In addition, anatase, apatite and rare kaolinite were formed during the alteration of the volcanic glass. Primary minerals including plagioclase show only minor textural evidence of alteration. However, some primary plagioclase laths show X-ray amorphous rims depleted in Na, Ca and Al. The TEM investigations of the dacitic lava samples from the PACMANUS vent field demonstrate that volcanic glass has a higher susceptibility to hydrothermal alteration at low temperatures than most associated primary phases. The findings of the study suggest that the interaction between the volcanic rock and the hydrothermal fluids proceeded under open-system conditions leading to a mobilization of alkali elements and a redistribution of Ti at the nm scale. The Mg required for the formation of trioctahedral smectite was supplied by the hydrothermal fluids.

 Key Words—Glass-smectite Conversion, Hydrothermal Alteration, PACMANUS Vent Field, Transmission Electron Microscopy.

INTRODUCTION

Glass contained in volcanic rocks is thermodynamically unstable and is more susceptible to alteration than most associated primary minerals. Therefore, initial alteration of glass-bearing volcanic rocks primarily involves the decomposition of the volcanic glass and the neoformation of glass alteration products (Steiner, 1968; Allen, 1988; Alt, 1995; Doyle, 2001; Gifkins and Allen, 2001). The results of previous investigations indicate that smectite is the principal glass alteration product at low temperatures although other phases, including zeolites and carbonates, may form, depending on temperature, reaction progress, the chemical composition and acidity of the aqueous fluids interacting with the volcanic glass, the fluid/rock ratio, the circulation regime of the fluids, and the glass chemical composition

(Hay and Iijima, 1968; Furnes and El-Anbaawy, 1980; Ghiara *et al.*, 1993; Tomita *et al.*, 1993; Alt *et al.*, 1998; De La Fuente *et al.*, 2002).

Previous studies have focused on the alteration of oceanic basalts to constrain the mechanisms of alteration and mineral neoformation taking place during the interaction of the oceanic crust and seawater (Andrews, 1980; Shau and Peacor, 1992; Giorgetti *et al.*, 2001; Zhou *et al.*, 2001; Alt and Teagle, 2003). The alteration of mafic volcanic glass at low temperatures is known to proceed through the formation of palagonite (Peacock, 1926), a mixture of amorphous to poorly crystalline phases. Although the chemical, mineralogical and structural nature of palagonite is debated, it is generally accepted that palagonite represents a transitional alteration product that transforms to fully crystalline phases including smectite during advanced alteration (Eggleton and Keller, 1982; Zhou and Fyfe, 1989; Jercinovic *et al.*, 1990; Zhou *et al.*, 1992; Stroncik and Schmincke, 2001).

In contrast to mid-ocean ridge basalts, relatively little is known about the mechanisms of low-temperature hydrothermal alteration of silicic lavas in the submarine environment (Alt *et al.*, 1998; Lackschewitz *et al.*, 2004). Detailed studies are almost exclusively limited to

fine-grained silicic volcaniclastic deposits (Masuda *et al.*, 1996; Marumo and Hattori, 1999) and experimentally altered equivalents (Kawano *et al.*, 1993; Tomita *et al.*, 1993; De La Fuente *et al.*, 2002). The results of these investigations suggest that silicic glasses commonly undergo processes of alteration similar to those acting on mafic volcanic glass where alteration proceeds through the formation of primitive precursors that evolve and grow to form secondary phases including smectite. Primitive clays have, for instance, been described by Masuda *et al.* (1996), Li *et al.* (1997) and Bauluz *et al.* (2002). These authors documented the occurrence of circular to elliptical structures with smectite-like compositions in volcanic glass that were found to be either not crystalline or of layered material with large (up to 10 nm), irregular periodicities. In contrast, silicic glass investigated by Tazaki *et al.* (1989) contained crystalline regions showing 0.3 nm domain structures within a truly non-crystalline matrix.

The present contribution focuses on the hydrothermal alteration of dacitic lava from the PACMANUS vent field in the eastern part of the Manus Basin, Papua New Guinea (Binns and Scott, 1993; Paulick *et al.*, 2004; Binns *et al.*, 2002). The alteration mineral associations occurring in the deep, high-temperature portion of this submarine geothermal system were found to be dominated by illite, chlorite and various mixed-layer phases (Lackschewitz *et al.*, 2004). In contrast, smectite is the principal glass alteration product forming in the upper, low-temperature portion of the submarine hydrothermal system (Binns *et al.*, 2002). Here, we present the results of a combined X-ray diffraction (XRD), scanning electron microscope (SEM) and TEM study that was carried out to characterize the products of low-temperature hydrothermal alteration of the dacitic glass sampled from the immediate subsurface of the PACMANUS vent field. High-resolution techniques were employed to study the products of the glass alteration and their textural relationships at the nm scale.

GEOLOGICAL SETTING

The geology of the PACMANUS hydrothermal vent field has recently been described by Binns *et al.* (2002). The submarine hydrothermal system is situated on Pual Ridge, a northeast-trending volcanic edifice that is 15 km long, 1−1.5 km wide, and rises ~500 m above the surrounding seafloor to a minimum water depth of ~1655 m. The ridge is primarily composed of glassy dacite, vesicular andesite and basaltic andesite (Binns and Scott, 1993; Paulick *et al.*, 2004). The main hydrothermal activity is restricted to a 2 km long section and is located between two low dacite knolls at the crest of the ridge. Seafloor observations revealed that the vent field comprises several discrete areas of hydrothermal activity, each measuring ~100−200 m in diameter (Figure 1).
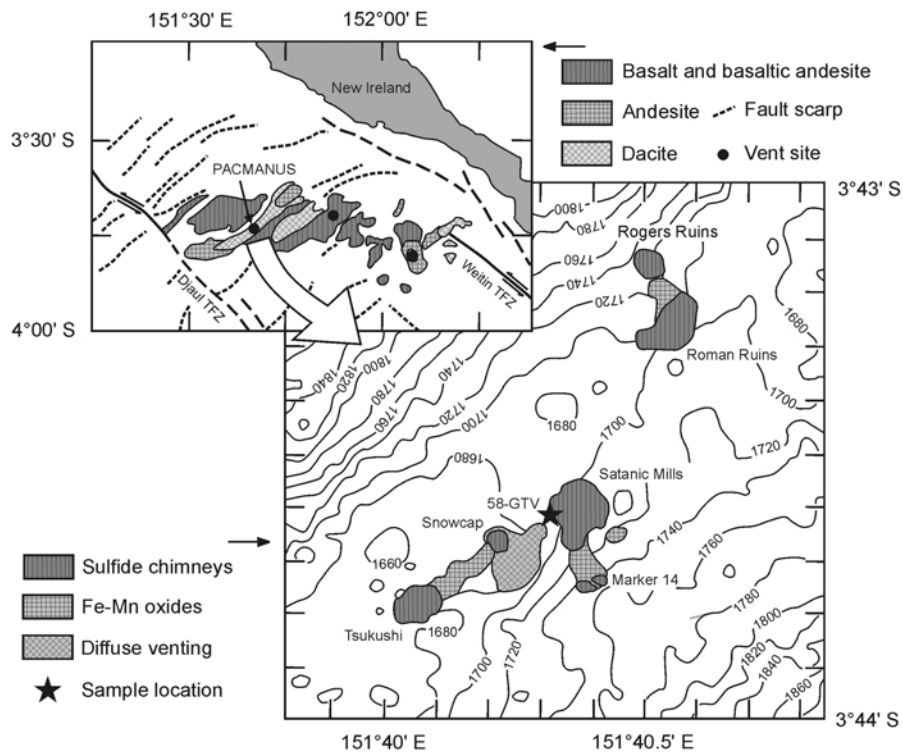

Figure 1. Distribution of hydrothermal deposits at the PACMANUS vent field. The map also gives the sampling location of the dacitic lava investigated in the present study. The inset shows the seafloor geology of the eastern Manus Basin (modified from Binns *et al.*, 2002).

Single, columnar sulfide chimneys and complex multispired structures consisting of active and extinct sulfide chimneys occur at the Roger Ruins, Roman Ruins and Satanic Mills vent sites (Moss and Scott, 2001; Binns *et al.*, 2002). Submersible dives showed that the temperatures of the clear hydrothermal fluids discharging at the orifices of the sulfide chimneys range from 220 to 276ºC (Auzende *et al.*, 1996; Gamo *et al.*, 1996; Douville *et al.*, 1999; Binns *et al.*, 2002). The hydrothermal fluids are unusually acidic (end-member pH values of 2.5 to 3.5 at 25ºC), show high K/Ca ratios reflecting equilibration with the dacite wallrocks, and are typified by high Mn and Fe contents when compared to hydrothermal systems at mid-ocean ridges (Auzende *et al.*, 1996; Douville *et al.*, 1999; Binns *et al.*, 2002).

In addition to the areas of high-temperature venting, diffuse discharge of low-temperature fluids (at ~6ºC) has been observed in the Snowcap area that is located several hundred meters to the southwest along Pual Ridge. The diffuse vent site is marked by conspicuous white bacterial mats (or possibly methane hydrate deposits). Several small fields of actively smoking and inactive chimneys have been located at the southwestern fringes of the Snowcap area (Binns and Scott, 1993; Binns *et al.*, 2002).

SAMPLE SELECTION AND EXPERIMENTAL METHODS

The samples were collected from the Satanic Mills vent site during cruise SO-166 of the German research vessel *Sonne* (Herzig *et al.*, 2003). Seafloor observations prior to sampling showed that the sampling area in the western part of the vent site (Figure 1) was dominated by small sulfide chimneys that were sited immediately on top of variably altered volcanic substrate. In addition to sphalerite-dominated black smoker chimneys and numerous chimney fragments, a number of dacite specimens was recovered using a TV-guided grab (station 58GTV at 3º43.62′S and 151º40.31′E; 1682 m below sea-level). The dacite specimens exhibited a range of alteration intensities. Apparently unaltered glassy dacite as well as altered equivalents containing abundant clay minerals were recovered.

Initially, optical microscopy and SEM were carried out to characterize the recovered samples using regular polished thin-sections. A Jeol JSM 6400 microscope, equipped with a Tracor (Noran) series II energy-dispersive X-ray spectrometer, was used at 20 kV and a beam current of 600 μA. Based on the results of the petrographic investigations, two representative samples containing abundant clay minerals (58GTV-4Q and 58GTV-4T) were chosen to study the conversion of volcanic glass to secondary phases in detail.

The two representative whole-rock samples were crushed and the <2 μm size fractions were separated by conventional gravity sedimentation. Step-scan XRD data

(5−80º2θ, 0.03º2θ step width, 8 s/step) were collected on the <2 μm size fractions using an URD 6 (Seifert-FPM) diffractometer that was equipped with a diffracted-beam graphite monochromator and a variable divergence slit allowing the irradiation of a constant area of the rotated standard random powder mounts. A Co tube was used and operated at 40 kV and 30 mA. Full-pattern fitting of the step scan data was performed using the fundamental-parameter Rietveld program BGMN (Bergmann *et al.*, 1998) employing a smectite real structure model developed by Ufer *et al.* (2004). The automatic refinement included the optimization of scale factors, lattice parameters, some occupancy factors and profile parameters for each phase as well as preferred orientation models for dioctahedral smectite, labradorite, pigeonite, magnetite, sphalerite and anatase together with background, zero point and sample displacement. In addition, oriented samples were prepared using the standard glass slide method. Step-scan data of these samples (2−16º2θ, 0.05º2θ step width, 10 s/step) were obtained after air drying, ethylene glycol solvating and heating at 550ºC for 2.4 h.

Sample preparation for the TEM and analytical electron microscope (AEM) investigations included the preparation of sticky wax-polished thin-sections of the two altered dacite samples. Initially, Cu discs with a central hole (600 μm diameter) were attached to the samples at texturally distinct sites (unaltered glassy groundmass, altered groundmass containing abundant clay minerals adjacent to fractures and vesicles). A total of six mounted samples were subsequently removed and ion-milled using a Gatan Duall Ion Mill 600. The TEM observations and AEM analyses were obtained using a Jeol 2010 microscope operated at 200 kV. The quantitative AEM analyses were carried out employing an X-ray energy dispersive system (EDS) Link Isis EDX and a beam diameter of ~20 nm. The AEM spectra were processed using k factors determined on natural ion-milled standards (paragonite, muscovite, albite, clinochlore, fayalite, rhodonite and titanite).

RESULTS

Petrographic and SEM observations

Petrographic investigations showed that the dacite samples from the Satanic Mills vent site contain minor (estimated <1 vol.%) microphenocrysts of plagioclase, clinopyroxene and magnetite. The glassy groundmass hosts abundant microlites (estimated ~30 vol.%) that are primarily composed of plagioclase. Clinopyroxene and magnetite microlites are less abundant. Apatite was found to be a rare primary accessory phase forming clusters of euhedral crystals in the glassy groundmass or rare inclusions in plagioclase microphenocrysts.

Hydrothermal alteration of the dacitic lava proceeded along networks of interconnected perlitic cracks and vesicles. The cracks and vesicles are typically enveloped

by a zone of intense hydrothermal alteration where the originally glassy matrix has been converted into fine-grained secondary phases. Contacts between these zones of intense alteration and the still glassy groundmass away from the perlitic cracks and vesicle walls vary from sharp to irregular (Figure 2a). Plagioclase micro-lites contained in the hydrothermally altered zones are texturally unaltered whereas clinopyroxene and magne-tite are sometimes replaced by fine-grained secondary minerals and pyrite, respectively. Small crystals of secondary apatite are abundant in the zones of intense hydrothermal alteration. In contrast to the volcanic glass contained in the groundmass of the dacitic lava, the microphenocrysts were apparently not affected by the hydrothermal alteration. Although plagioclase micro-

Figure 2. Back-scattered electron images obtained of the altered dacite samples: (a) contact between a zone of intense hydro-thermal alteration adjacent to a perlitic fracture and the unaltered glassy groundmass. The formerly glassy matrix is partially converted to smectite (sm) close to the fracture whereas unaltered glass (gl) occurs away from the fluid pathway. The matrix contains abundant lath-shaped plagioclase (plg) and some pyroxene (pyx) microlites. Note that the contrast between the plagioclase microlites and the surrounding matrix is enhanced in the zone of intense hydrothermal alteration. (b) Plagioclase microphenocryst (plg) set in an intensely altered groundmass containing abundant smectite (sm) and lath-shaped plagioclase microlites. Note that the microphenocryst is intensely fractured; locally, sphalerite (sp) has precipitated along the fractures.

phenocrysts intersected by perlitic cracks are fractured and surrounded by the intensely altered groundmass, the microphenocrysts lack textural evidence of alteration (Figure 2b).

The hydrothermally altered dacite samples contain abundant sphalerite, pyrite, chalcopyrite and pyrrhotite. These phases typically precipitated within the perlitic cracks and vesicles. In addition, rare marcasite, galena, bornite and covellite have been recognized. Barite laths infilling vesicles are relatively common.

XRD data

X-ray diffraction analyses of the <2 μm fractions reveal that smectite is the dominant clay mineral in both samples investigated. Diffraction patterns collected on the oriented but untreated samples show broad and overlapping peaks at $12.4-14.5$ Å which shift to 17 Å upon ethylene glycol solvation (second-order reflection at 8.5 Å) and to 9.6 Å after heating at 550ºC (Figure 3). This behavior is characteristic of smectite whereby the broad first-order peak is caused by non-uniform basal distances, presumably related to the presence of variable amounts of interlayer water molecules. The samples contain trace amounts of kaolinite as suggested by the presence of sharp, but very weak reflections at 7.1 Å that disappear upon heating at 550ºC (Figure 3).

The XRD patterns of the random powder mounts show that the smectite is dominantly dioctahedral in nature. A pronounced 06,33 reflection is located at ~1.49 Å. However, an additional small peak is observed at 1.53 Å which is interpreted to be the 06,33 reflection of a trioctahedral smectite species that is only present in minor amounts. Full-pattern fitting of the XRD patterns confirmed that the small peak at 1.49 Å cannot be accounted for by models assuming only the presence of dioctahedral smectite in addition to labradorite, pigeo-nite, magnetite, sphalerite and anatase (Figure 4). Rietveld analysis also showed that anatase is present in significant amounts in the <2 μm fractions of the altered samples, a phase that was not identified in thin-section by optical microscopy and SEM.

TEM observations and AEM analyses

The TEM observations were performed in zones of intense hydrothermal alteration surrounding perlitic cracks and vesicles as well as on the glassy groundmass away from fluid pathways. In general, the textures of the ion-milled samples were found to be similar for the altered and unaltered sites investigated in both dacite samples.

The alteration intensity of the glassy groundmass varies substantially over short distances. Figure 5 shows a TEM image of unaltered volcanic glass located between two adjacent lath-shaped plagioclase crystals. The unaltered glass is apparently homogeneous and hosts numerous small (~20 nm) prismatic to round pyroxene crystals. The AEM analyses show that the

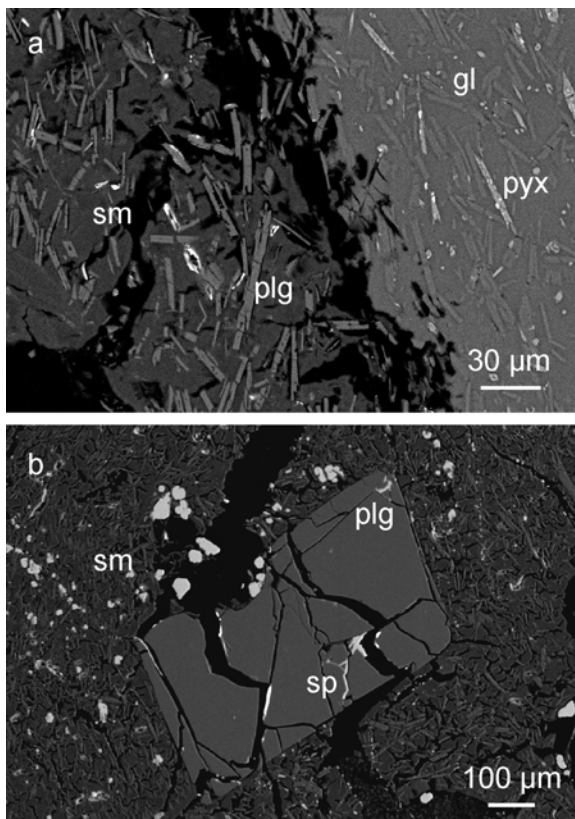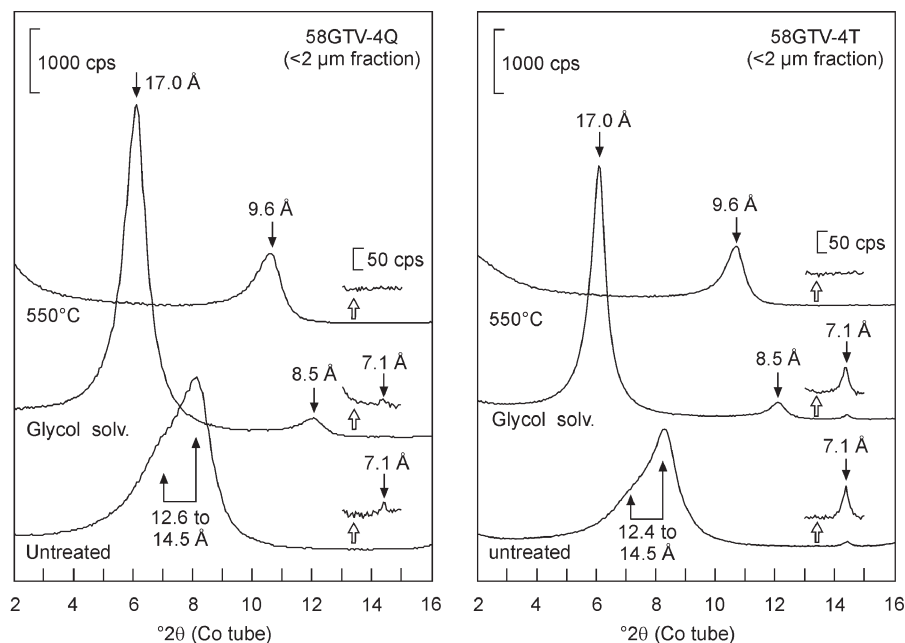Figure 3. XRD patterns (oriented mounts) of the <2 μm fractions of the two dacite samples. The samples contain substantial amounts of smectite (basal reflections: untreated = 12.4–14.5 Å, ethylene glycol solvated = 17 Å and 8.5 Å, heated to 550°C = 9.6 Å) and traces of kaolinite (basal reflection: untreated = 7.1 Å, not observed after heating to 550°C).

unaltered volcanic glass is primarily composed of Si, with smaller amounts of Al, Fe, Na, Ca, K and traces of Mg and Ti. The glass is homogeneous in composition

(Table 1). Several micrometers away from the unaltered area, the volcanic glass has been affected by hydro-thermal alteration (Figure 6a). The transition zone
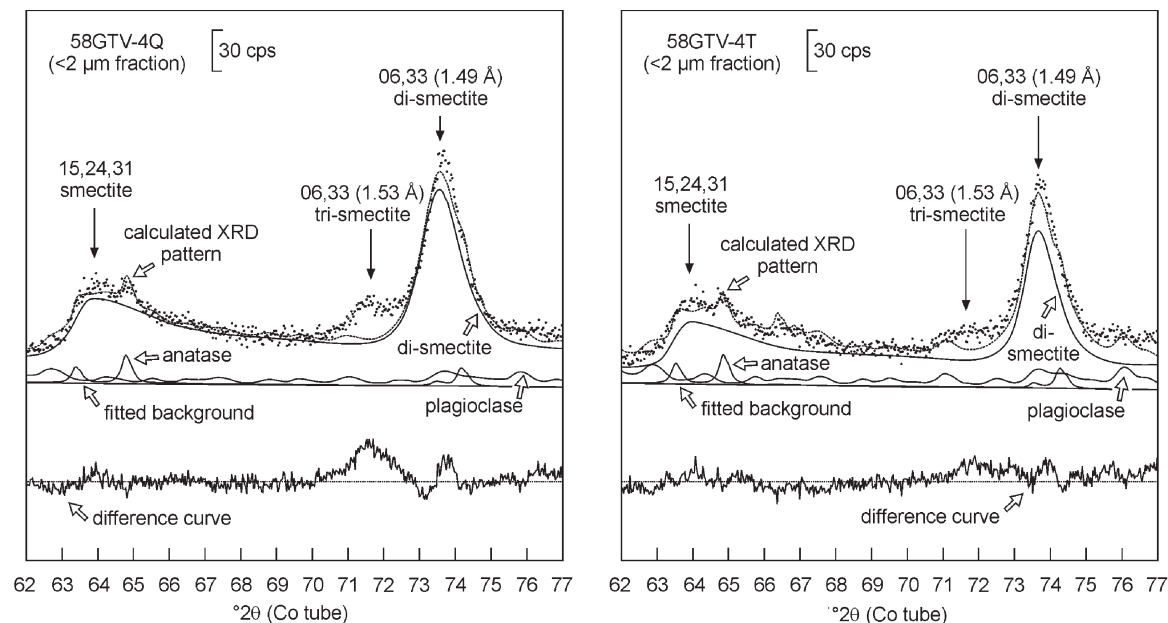
Figure 4. XRD patterns (random powder mounts) of the <2 μm fractions of the two dacite samples. Full-pattern fitting of the step-scan data has been performed by the Rietveld method assuming the presence of dioctahedral smectite in addition to labradorite, pigeonite, magnetite, sphalerite and anatase (points = measured data, dotted line = fitted XRD profile). The calculated profiles of anatase, plagioclase and dioctahedral smectite are given for comparison whereas those of the other phases were omitted for clarity. Note that no close agreement between the observed data and the calculated profile could be obtained assuming dioctahedral smectite to be the only sheet silicate present. The difference between the measured and modelled intensities (solid line in the lower part of the diagram is the difference curve) suggests the existence of a weak reflection at 1.53 Å. This peak is interpreted to be the 06,33 reflection of a trioctahedral smectite species.

Figure 5. TEM image of plagioclase (plg) embedded in unaltered volcanic glass (gl). The glassy matrix contains abundant prismatic to round pyroxene crystals (pyx).

between unaltered and altered glass is ~200 nm wide and characterized by a marked increase in the pore density. The hydrothermally altered glass contains abundant, up to 10 nm thick, flakes of smectite that have random orientations. In many cases, the curved and irregularly shaped smectitic flakes partially fill or coat the round cavities present in the altered glass. Figure 6b shows that the smectitic flakes display 00l lattice fringes that are wavy and of variable spacing (1.1−1.5 nm), a feature that is characteristic of dehydrated, collapsed smectite in the high-vacuum environment (Peacor, 1992).

Zones of intense hydrothermal alteration adjacent to perlitic fractures and vesicles lack volcanic glass and are largely composed of cavities and smectitic flakes. In these areas, the smectite forms bent crystals that have random orientations (Figure 7). The 00l lattice fringes of the smectitic flakes are wavy and highly defective, with abundant layer terminations. The thickness of the flakes rarely exceeds 40 nm with an average thickness of ~14−15 nm. No selected area electron diffraction patterns (SAED) could be obtained from the smectitic flakes.

Representative AEM analyses of smectite contained in the two altered samples are listed in Table 2; the data

are given in atoms per $O_{20}(OH)_4$. Due to the small sizes of the smectite crystals, analyses could only be obtained in areas where several smectite flakes are closely intergrown. In most cases, three to four differently oriented smectite flakes contributed to each AEM analysis.

Most smectite flakes analyzed are of dioctahedral composition. The total of the octahedral cations ranges from 3.8 to 4.4 atoms per formula unit (a.p.f.u.). The AEM analyses indicate that the dioctahedral smectite belongs to the montmorillonite–beidellite series (Figure 8). The Mg content of the dioctahedral smectite broadly increases with proximity to fluid pathways. Smectite flakes hosted by the altered glassy matrix away from the perlitic fractures and vesicles have small Mg contents (<0.3 a.p.f.u.) whereas smectitic flakes located in zones of intense hydrothermal alteration adjacent to fractures and vesicles have distinctly larger Mg contents (>0.5 a.p.f.u.). Sodium and K represent the principal interlayer cations in the dioctahedral smectite. Most smectitic flakes analyzed are typified by an interlayer cation content of <1.0 a.p.f.u. and K/Na ratios of <1. In general, smectite flakes contained in the zones of intense hydrothermal alteration adjacent to the perlitic fractures have the largest K contents. However, rare smectitic flakes hosted by the altered glassy groundmass away from the fluid pathways exhibit compositions approaching that of illite. The interlayer cation content of these flakes exceeds 1.2 a.p.f.u. with a K concentration that is close to 1.0 a.p.f.u. (Table 2).

In some cases, smectitic flakes having trioctahedral compositions corresponding to saponite (Figure 8) occur in zones of intense hydrothermal alteration adjacent to the perlitic cracks and vesicles. In these flakes, the total of the octahedral cations exceeds 4.0 a.p.f.u., with a Mg content >2.0 a.p.f.u. The small total of octahedral cations (4.6−5.1 a.p.f.u.) probably indicates that the smectite flakes were too small to be analyzed and that some volcanic glass contributed to the AEM analyses. Table 2 shows that Na and K are the dominant interlayer cations in the saponite. The trioctahedral smectite (Figure 9) is texturally indistinguishable from the more

Table 1. AEM analyses (wt.%) of unaltered volcanic glass in the dacite samples from the PACMANUS hydrothermal vent field.

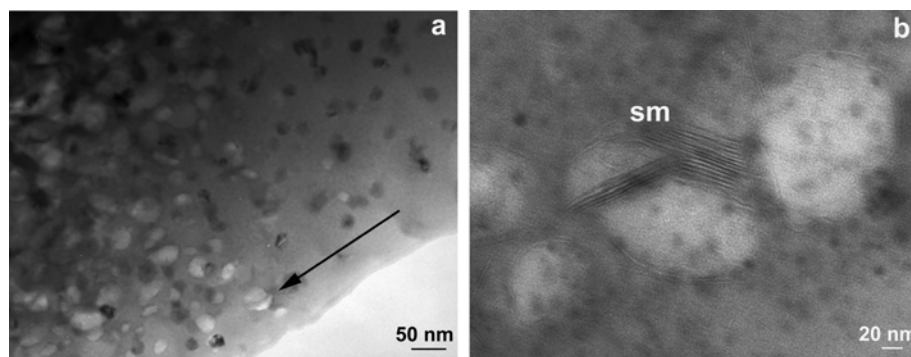| | 58GTV-4Q | | | 58GTV-4T | | |
	1	2	3	4	5	6
SiO_2	74.30	75.23	75.90	75.12	75.38	73.84
TiO_2	0.67	0.73	0.81	0.94	0.76	0.83
Al_2O_3	12.37	12.34	12.45	12.20	12.46	12.39
Fe_2O_3	4.37	3.72	4.35	4.45	3.69	3.92
MgO	1.23	1.05	0.98	1.19	0.90	1.04
CaO	2.02	2.10	1.37	2.00	1.77	1.92
Na_2O	2.53	2.45	2.31	2.40	2.49	3.95
K_2O	2.51	2.38	1.83	1.70	2.55	2.11
Σ	100.00	100.00	100.00	100.00	100.00	100.00

Figure 6. TEM images of the intensely altered dacite samples. (a) Transition zone between unaltered and altered glass. The arrow indicates the direction of the transition. The unaltered glass contains abundant $10-20$ nm crystals composed of magnetite or hematite (dark crystals). The altered glass is typified by the occurrence of pores that appear as white spots in the image. (b) A round cavity in the altered glass is coated by a bent flake of smectite (sm) that is only a few layers thick (~7 to 8 nm).

frequently occurring dioctahedral species. The saponite also forms bent and randomly oriented flakes replacing the volcanic glass. The sizes of the flakes are comparable to those having compositions corresponding to montmorillonite-beidellite.

In addition to smectite, hydrothermal alteration resulted in the formation of abundant anhedral crystals that are $30-40$ nm in size. These crystals display straight lattice fringes with a spacing of 0.37 nm (Figure 10). The EDS spectra show that these crystals are principally composed of TiO_2. The structural and chemical characteristics suggest that these crystals correspond to the anatase detected by the XRD experiments. In several locations, the smectite was also found to be associated with rare crystals having 0.7 nm-spaced, regular lattice fringes (Figure 10). Because these crystals are too small (~10 nm thick) to be analyzed by the AEM technique used, information on the composition of this phase could not be gathered. However, the results of the XRD investigations suggest that the phase with the

0.7 nm-spaced lattice fringes represents kaolinite. In addition to anatase and kaolinite, zones of intense hydrothermal alteration adjacent to perlitic fractures and vesicles contain prismatic apatite crystals that have sizes of ~30 nm $\times$ 250 nm. Because the abundance of apatite decreases with increasing distance from fractures and vesicles, the apatite is also interpreted to be secondary in origin.

The TEM observations confirm that primary minerals contained in the altered dacite samples are texturally unmodified by the hydrothermal alteration. Secondary phases are usually only present in the glassy matrix surrounding primary plagioclase microlites and microphenocrysts and do not show any textural relations with them. No plagioclase replacement by smectite or other clay minerals has been observed. However, several
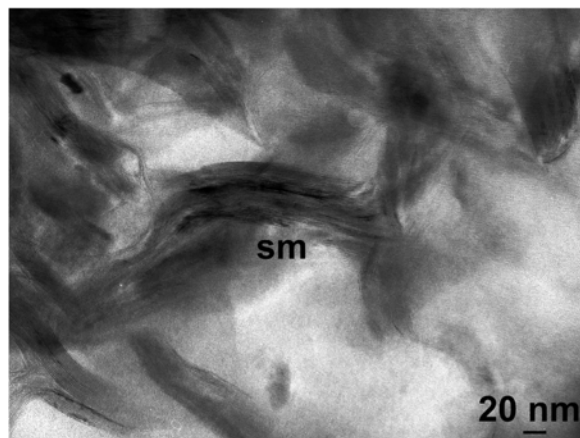
Figure 7. TEM image of intensely altered groundmass that contains smectitic flakes (sm) up to 30 nm thick. The crystals are randomly oriented and bent. The lattice fringes are highly defective and show a variable spacing of 1.0 to 1.5 nm.
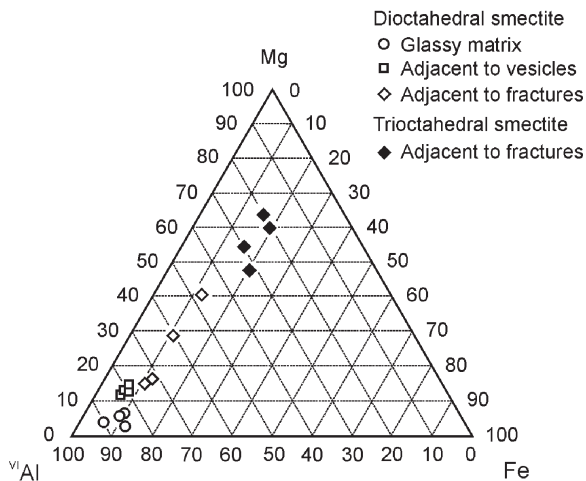

Figure 8. Compositional variations of smectitic flakes occurring in texturally distinct settings in the two intensely altered dacite samples (see text for discussion). The triangular plot illustrates the relative importance of different cations occupying the octahedral positions in the smectite structure (see text for discussion). All Fe was treated as Fe^{3+}. Formulae were calculated on the basis of $O_{20}(OH)_4$.

Table 2. AEM analyses of smectitic flakes contained in intensely altered dacite samples from the PACMANUS hydrothermal vent field. Compositions are given in atoms per $O_{20}(OH)_4$.

	Dioctahedral smectite												Trioctahedral smectite			
	1	2	3	4	5	6	7	8	9	10	11	12	13	14	15	16
Si	7.50	7.58	7.79	7.65	7.67	7.65	7.84	7.78	7.64	7.66	7.57	7.34	7.03	6.96	7.15	6.91
^{IV}Al	0.50	0.42	0.21	0.35	0.33	0.35	0.16	0.22	0.36	0.34	0.43	0.66	0.97	1.04	0.85	1.09
^{VI}Al	3.60	3.39	3.34	3.26	3.23	3.25	3.27	3.30	2.93	2.47	2.04	2.76	1.46	1.34	1.00	0.92
Ti	0.06	n.d.	0.03	n.d.	n.d.	n.d.	n.d.	n.d.	0.07	n.d.	n.d.	0.23	0.12	0.47	0.16	0.44
Mg	0.18	0.25	0.29	0.13	0.58	0.65	0.54	0.58	0.64	1.22	1.85	0.66	2.65	2.01	3.18	2.72
Fe	0.23	0.36	0.37	0.44	0.27	0.24	0.20	0.23	0.39	0.40	0.50	0.42	0.70	0.79	0.77	0.82
Mn	n.d.	n.d.	n.d.	n.d.	n.d.	n.d.	n.d.	n.d.	n.d.	n.d.	n.d.	n.d.	n.d.	n.d.	n.d.	n.d.
Na	0.33	0.27	0.18	0.30	0.40	0.34	0.41	0.42	0.41	0.38	n.d.	0.29	0.19	n.d.	0.17	0.24
Ca	n.d.	n.d.	n.d.	0.12	n.d.	n.d.	n.d.	n.d.	n.d.	0.31	0.12	0.05	0.09	0.11	0.05	0.06
K	0.07	0.11	0.13	0.85	0.14	0.12	0.19	0.07	0.31	0.24	0.37	0.49	0.30	0.36	0.22	0.28
ΣVI	4.07	4.00	4.03	3.83	4.08	4.14	4.01	4.11	4.03	4.09	4.39	4.07	4.93	4.61	5.11	4.90
ΣXII	0.40	0.38	0.31	1.27	0.54	0.46	0.60	0.49	0.72	0.93	0.49	0.83	0.58	0.47	0.44	0.58
$^{VI}Al+Fe$	3.83	3.75	3.71	3.70	3.50	3.49	3.47	3.53	3.32	2.87	2.54	3.18	2.16	2.13	1.77	1.74
Fe+Mg	0.41	0.61	0.66	0.57	0.85	0.89	0.74	0.81	1.03	1.62	2.35	1.08	3.35	2.80	3.95	3.54

Chemical analyses were obtained on flakes contained in altered glassy matrix (1−4), in zones of intense hydrothermal alteration adjacent to vesicles (5−8) and in perlitic cracks (9−16).
All Fe was treated as Fe^{3+}
n.d. = not detected
ΣVI = sum of octahedral cations
ΣXII = sum of interlayer cations

plagioclase microlites and microphenocrysts show an ~70−100 nm thick amorphous rim enveloping the apparently unaltered core (Figure 11). The EDS spectra show that the amorphous rim has markedly smaller Na, Ca and Al contents when compared to the unaltered plagioclase (Figure 12a,b).

DISCUSSION

The results of the present investigation show that smectite with compositions corresponding to beidellite-montmorillonite 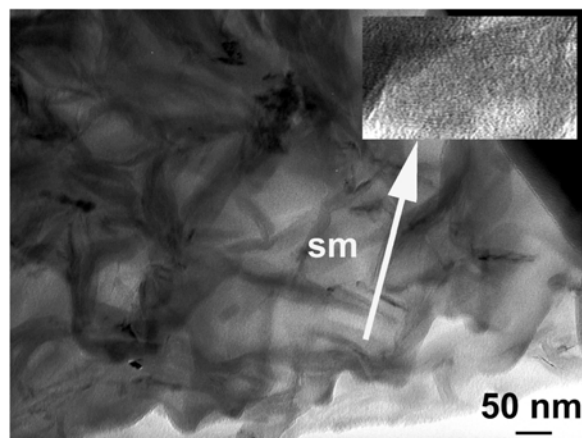is the principal product of hydrothermal alteration forming in the immediate subsurface of the submarine PACMANUS hydrothermal vent field. The abundant presence of smectite indicates that alteration proceeded at relatively low temperatures. Conversion to illite through the formation of mixed-layer illite-smectite is initiated at temperatures of ~150ºC in most geothermal systems (Steiner, 1968; Elders *et al.*, 1981; Harvey and Browne, 1991; Inoue *et al.*, 1992; Cox and Browne, 1998) and takes place over a broad temperature interval

Figure 9. TEM image showing randomly oriented and bent trioctahedral smectitic flakes (sm) with defective lattice fringes having variable spacings.
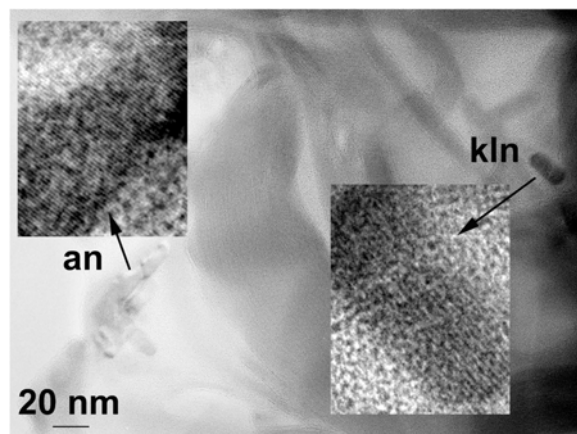

Figure 10. TEM image showing one small kaolinite crystal (kln) and one anatase crystal (an) within the smectite-bearing groundmass of the intensely altered dacite. The insets give the enlarged lattice-fringe images of kaolinite with 0.7 nm-spaced lattice fringes and of anatase that has 0.37 nm spaced lattice fringes.
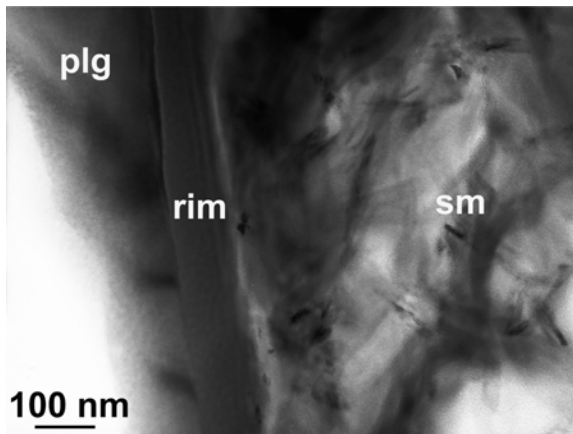
Figure 11. TEM image of a plagioclase crystal (plg) that is surrounded by a ~70 nm thick X-ray amorphous rim depleted in Na, Ca and Al. The plagioclase crystal is surrounded by a groundmass consisting of randomly oriented smectitic flakes (sm).

that varies as function of kinetically controlled processes of reaction progress (Essene and Peacor, 1995).

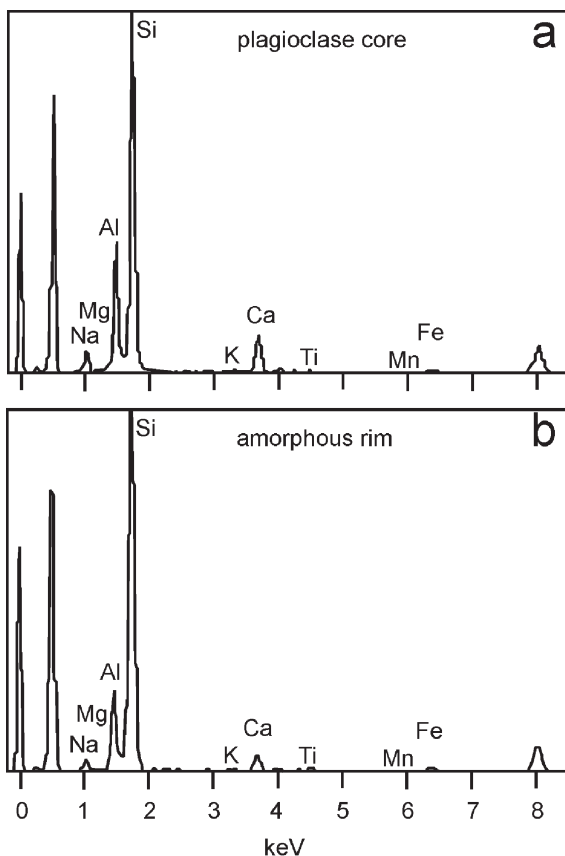Although previous studies have shown that smectite is a common low-temperature hydrothermal alteration

Figure 12. EDS spectra collected on the plagioclase crystal shown in Figure 11. (a) Spectrum of the unaltered plagioclase core. (b) Spectrum of the X-ray amorphous rim surrounding the plagioclase core.

product of volcanic glass, the processes of smectite neoformation at the PACMANUS hydrothermal vent field are different from those previously described. In contrast to the findings of Eggleton and Keller (1982), Zhou and Fyfe (1989), Tazaki *et al.* (1989), Zhou *et al.* (1992), Kawano *et al.* (1993), Masuda *et al.* (1996), Li *et al.* (1997) and Bauluz *et al.* (2002), no amorphous precursors or primitive clays have been detected in the altered dacite samples. The volcanic glass appears to have transformed directly to smectite through a dissolution and precipitation process without the formation of a metastable intermediate phase. The major chemical constituents were mobilized, at least locally, during the dissolution of glass to form smectite. The resultant textures are similar to those described by Banfield *et al.* (1991). Randomly oriented smectitic flakes fill or coat the walls of round cavities and pores forming during the dissolution of the volcanic glass. The observed variations in the interlayer cation occupancy suggest that the precipitation of smectite having low Na/K ratios was promoted in zones of intense hydrothermal alteration whereas smectite with elevated Na/K ratios occurs more frequently away from the fluid pathways. These systematic variations suggest that solution transport of alkali elements represents an important factor controlling the composition of the glass alteration products at PACMANUS.

In addition to dioctahedral smectite with a low Na/K interlayer cation ratio, zones of intense hydrothermal alteration around perlitic cracks and vesicles were found to contain Mg-rich, trioctahedral smectite with compositions close to saponite. Saponite represents the most common secondary mineral forming during low-temperature alteration of oceanic basalts (Alt, 1999) where substantial amounts of Fe and Mg are liberated during the breakdown of primary phases such as olivine and pyroxene. In contrast to oceanic basalts, neoformation of saponite at PACMANUS required the influx of Mg from the hydrothermal fluids because the unaltered silicic volcanic rocks only contain small amounts of MgO concentrations (Paulick *et al.*, 2004; Lackschewitz *et al.*, 2004). The observations at the nanoscale show that the trioctahedral smectite contained in the altered groundmass has textures similar to those observed for the dioctahedral species. Consequently, the saponite is interpreted to have formed by a similar process of dissolution and crystallization from the volcanic glass involving an aqueous fluid as a transport medium and source of Mg although direct precipitation from the fluids as suggested by Fiore *et al.* (2001) cannot be ruled out conclusively. The observation that the occurrence of trioctahedral smectite flakes is largely confined to areas of intense alteration suggests that the relative abundance of Mg-rich smectite increases as alteration of the volcanic glass proceeds, a fact also documented in other natural and experimental systems (Fiore *et al.*, 2001; Caballero *et al.*, 1991).

The observations of the present study further suggest that alteration of the silicic glass resulted in the formation of secondary anatase. Studies on authigenic anatase indicate that this TiO_2 polymorph forms in different rock types at low temperature as a metastable phase with respect to rutile (Post and Burnham, 1986). Direct precipitation of anatase from hydrothermal solutions has been observed in the Salton Sea geothermal field. At this location, anatase forms euhedral crystals in the pore space of the host sedimentary rocks. The anatase precipitated at temperatures of $115-260°C$ in response to the release of Ti during the conversion of smectite to illite (Yau *et al.*, 1987). Anatase also represents a frequent alteration product of primary Ti-bearing oxides and silicates and in this case usually occurs in textural association with remnants of the precursor mineral at the nanometer scale. For instance, in a detailed TEM study on weathered perovskite, Banfield and Veblen (1992) established that anatase formed by topotactic replacement of the host material. The anatase was found to be separated from the perovskite precursor by a very narrow zone (<1 nm) marking a region of structural reorganization. Similarly, Tilley and Eggleton (2005) showed that anatase formed as an alteration product of titanite by a process of local dissolution-precipitation. In the samples investigated in the present study, anatase forms crystals several nm in width within the altered groundmass and there is no textural or spatial relations with a primary Ti-bearing phase. The constant size and the euhedral shape of the crystals indicate that the anatase precipitated as a result of the short-range mobilization of Ti liberated during the glass alteration.

Hydrothermal alteration of the dacite lava was accompanied by the formation of trace amounts of kaolinite despite the fact that smectite represents the principal alteration product in the immediate subseafloor of the PACMANUS vent field. Both secondary phases appear to have formed broadly contemporaneously from the volcanic glass; overprinting relationships indicative of the formation of kaolinite and smectite at different alteration conditions have not been observed. The formation of kaolinite at conditions generally promoting the conversion of volcanic glass to smectite is interpreted to result from kinetic controls on mineral neoformation, although local variations in the composition of the relatively acidic hydrothermal fluids interacting with the dacitic lava cannot be ruled out.

The high-resolution TEM observations show that the secondary minerals forming during the hydrothermal alteration primarily replace the volcanic glass contained in the groundmass of the dacitic lava samples. This finding is in agreement with the observations of the optical and scanning electron microscopic investigations demonstrating that the volcanic glass was more susceptible to alteration than the primary phases contained in the lava. However, the TEM study demonstrates that

plagioclase microphenocrysts and microlites exhibit amorphous rims where Na, Ca and Al have been lost during hydrothermal alteration. Thus, even the apparently most resistant phases contained in the dacitic rocks investigated were involved in alteration processes although susceptibility to alteration varied greatly among the individual phases.

The conversion of the volcanic glass to secondary minerals including beidellite-montmorillonite, saponite, anatase and kaolinite occurred in an environment of steep temperature gradients. Low-temperature alteration allowing the formation of abundant smectite appears to be restricted to the immediate subsurface of the PACMANUS hydrothermal vent field whereas high-temperature alteration, causing the precipitation of illite, chlorite and various mixed-layer phases, takes place at depth in the upflow zones of the hydrothermal fluids (Lackschewitz *et al.*, 2004). Alteration of the volcanic glass contained in dacitic lavas proceeded under open-system conditions as shown by the behavior of the alkali elements during glass alteration and the uptake of Mg from the hydrothermal fluids during saponite formation. The hydrothermal alteration occurred in an environment that promoted the precipitation of secondary minerals without the formation of metastable transitional phases.

CONCLUSIONS

The results of this study suggest that the kinetics of glass dissolution and mineral formation are distinct at the PACMANUS hydrothermal vent field. Low-temperature alteration of silicic volcanic glass under near-seafloor open system submarine geothermal conditions resulted in the formation of abundant di- and tri-octahedral smectite, but was not associated with the formation of poorly crystalline precursor phases. The glass alteration involved a solution transport of alkali and earth alkali elements. The formation of smectite coincided with a mobilization of Na from the glassy dacite and the addition of significant amounts of Mg from the hydrothermal fluids. The analytical electron microscope investigations revealed that the composition of smectite is linked to the extent of glass-fluid interaction at the micron scale. As alteration proceeds, K liberated during glass alteration, or supplied by the hydrothermal fluids, is preferentially taken up by the newly formed smectite causing a systematic shift in the interlayer occupancy. Addition of Mg to the sites of alteration resulted in the formation of saponite close to fluid pathways. The presence of newly formed anatase is indicative of a local redistribution of Ti originally contained in the unaltered volcanic glass.

REFERENCES

Allen, R.L. (1988) False pyroclastic textures in altered silicic lavas, with implications for volcanic-associated mineralization. *Economic Geology*, **83**, 1424−1446.

Alt, J.C. (1995) Subseafloor processes in mid-ocean ridge hydrothermal systems. Pp. 85−114 in: *Seafloor Hydrothermal Systems: Physical, Chemical, Biological and Geological Interactions* (S.E. Humphris, R.A. Zierenberg, L.S. Mullineaux and R.E. Thomson, editors). Geophysical Monograph Series, **91**. American Geophysical Union, Washington.

Alt, J.C. (1999) Very low-grade hydrothermal metamorphism of basic igneous rocks. Pp. 169−201 in: *Low-grade Metamorphism* (M. Frey and M. Robinson, editors). Blackwell Science, Oxford, UK.

Alt, J.C. and Teagle, D.A.H. (2003) Hydrothermal alteration of upper oceanic crust formed at a fast-spreading ridge: Mineral, chemical, and isotopic evidence from ODP Site 801. *Chemical Geology*, **201**, 191−211.

Alt, J.C., Teagle, D.A.H., Brewer, T., Shanks, W.C., III and Halliday, A. (1998) Alteration and mineralization of an oceanic forearc and the ophiolite-ocean crust analogy. *Journal of Geophysical Research*, **B103**, 12365−12380.

Andrews, A.J. (1980) Saponite and celadonite in layer 2 basalts, DSDP Leg 37. *Contributions to Mineralogy and Petrology*, **73**, 323−340.

Auzende, J.M., Urabe, T. and Shipboard Scientific Party (1996) Cruise explores hydrothermal vents of the Manus Basin. *EOS Transactions of the American Geophysical Union*, **77**, 244.

Banfield, J.F. and Veblen, D.R. (1992) Conversion of perovskite to anatase and TiO_2 (B): A TEM study and the use of fundamental building blocks for understanding relationships among the TiO_2 minerals. *American Mineralogist*, **77**, 545−557.

Banfield, J.F., Jones, B.F. and Veblen, D.R. (1991) An AEM-TEM study of weathering and diagenesis, Albert Lake, Oregon: I. Weathering reactions in the volcanics. *Geochimica et Cosmochimica Acta*, **55**, 2781−2793.

Bauluz, B., Peacor, D.R. and Ylagan, R.F. (2002) Transmission electron microscopy study of smectite illitization during hydrothermal alteration of a rhyolitic hyaloclastite from Ponza, Italy. *Clays and Clay Minerals*, **50**, 157−173.

Bergmann, J., Friedel, P. and Kleeberg, R. (1998) BGMN − A new fundamental parameters-based Rietveld program for laboratory X-ray sources, its use in quantitative analysis and structure investigations. *CPD Newsletter*, **20**, 5−8.

Binns, R.A. and Scott, S.D. (1993) Actively forming polymetallic sulfide deposits associated with felsic volcanic rocks in the eastern Manus back-arc basin, Papua New Guinea. *Economic Geology*, **88**, 2226−2236.

Binns, R.A., Barriga, F.J.A.S., Miller, D.J. and Shipboard Scientific Party (2002) Leg 193 summary. Anatomy of an active felsic-hosted hydrothermal system, Eastern Manus

Basin. *Proceedings of the Ocean Drilling Program, Initial Reports*, **193**, 1−84.

Caballero, E., Reyes, E., Huertas, F., Linares, J. and Pozzuoli, A. (1991) Early-stage smectites from pyroclastic rocks of Almeria (Spain). *Chemical Geology*, **89**, 353−358.

Cox, M.E. and Browne, P. (1998) Hydrothermal alteration mineralogy as an indicator of hydrology at the Ngawha geothermal field, New Zealand. *Geothermics*, **27**, 259−270.

De La Fuente, S., Cuadros, J. and Linares, J. (2002) Early stages of volcanic tuff alteration in hydrothermal experiments: Formation of mixed-layer illite-smectite. *Clays and Clay Minerals*, **50**, 578−590.

Douville, E., Bienvenu, P., Charlou, J.L., Donval, J.P., Fouquet, Y., Appriou, P. and Gamo, T. (1999) Yttrium and rare earth elements in fluids from various deep-sea hydrothermal systems. *Geochimica et Cosmochimica Acta*, **63**, 627−643.

Doyle, M.G. (2001) Volcanic influences on hydrothermal and diagenetic alteration: Evidence from Highway-Reward, Mount Windsor Subprovince, Australia. *Economic Geology*, **96**, 1133−1148.

Eggleton, R.A. and Keller, J. (1982) The palagonitization of limburgite glass − a TEM study. *Neues Jahrbuch für Mineralogie Monatshefte*, 321−336.

Elders, W.A., Hoagland, J.R. and Williams, A.E. (1981) Distribution of hydrothermal mineral zones in the Cerro Prieto geothermal field of Baja California, Mexico. *Geothermics*, **10**, 245−253.

Essene, E.J. and Peacor, D.R. (1995) Clay mineral thermometry − a critical perspective. *Clays and Clay Minerals*, **43**, 540−553.

Fiore, S., Huertas, F.J., Huertas, F. and Linares, J. (2001) Smectite formation in rhyolitic obsidian as inferred by microscopic (SEM-TEM-AEM) investigation. *Clay Minerals*, **36**, 489−500.

Furnes, H. and El-Anbaawy, M.I.H. (1980) Chemical changes and authigenic mineral formation during palagonitization of a basanite hyaloclastite, Gran Canaria, Canary Islands. *Neues Jahrbuch für Mineralogie Abhandlungen*, **139**, 279−302.

Gamo, T., Okamura, K., Kodama, Y. and Shipboard Scientific Party (1996) Chemical characteristics of hydrothermal fluids from the Manus back-arc basin, Papua New Guinea, I. Major chemical components. *EOS Transactions of the American Geophysical Union*, **77**, W116.

Ghiara, M.R., Franco, E., Petti, C., Stanzione, D. and Valentino, G.M. (1993) Hydrothermal interaction between basaltic glass, deionized water and seawater. *Chemical Geology*, **104**, 125−138.

Gifkins, C.C. and Allen, R.L. (2001) Textural and chemical characteristics of diagenetic and hydrothermal alteration in glassy volcanic rocks: Examples from the Mount Read Volcanics, Tasmania. *Economic Geology*, **96**, 973−1002.

Giorgetti, G., Marescotti, P., Cabella, R. and Lucchetti, G. (2001) Clay mineral mixtures as alteration products in pillow basalts from the eastern flank of Juan de Fuca Ridge: A TEM-AEM study. *Clay Minerals*, **36**, 75−91.

Harvey, C.C. and Browne, P.R.L. (1991) Mixed-layer clay geothermometry in the Wairakei geothermal field, New Zealand. *Clays and Clay Minerals*, **39**, 614−621.

Hay, R.L. and Iijima, A. (1968) Nature and origin of palagonite tuffs of the Honolulu Group on Oahu, Hawaii. *Memoir of the Geological Society of America*, **116**, 331−376.

Herzig, P.M., Petersen, S., Kuhn, T. and Shipboard Scientific Party (2003) Shallow drilling of seafloor hydrothermal systems using *R/V Sonne* and the BGS Rockdrill: Conical Seamount (New Ireland Fore-Arc) and Pacmanus (Eastern Manus Basin), Papua New Guinea. *InterRidge News*, **12**, 22−26.

Inoue, A., Utada, M. and Wakita, K. (1992) Smectite-to-illite conversion in natural hydrothermal systems. *Applied Clay Science*, **7**, 131−145.

Jercinovic, M.J., Keil, K., Smith, M.R. and Schmitt, R.A. (1990) Alteration of basaltic glasses from north-central British Columbia, Canada. *Geochimica et Cosmochimica Acta*, **54**, 2679−2696.

Kawano, M., Tomita, K. and Kamino, Y. (1993) Formation of clay minerals during low temperature experimental alteration of obsidian. *Clays and Clay Minerals*, **41**, 431−441.

Lackschewitz, K.S., Devey, C.W., Stoffers, P., Botz, R., Eisenhauer, A., Kummetz, M., Schmidt, M. and Singer, A. (2004) Mineralogical, geochemical and isotopic characteristics of hydrothermal alteration processes in the active, submarine, felsic-hosted PACMANUS field, Manus Basin, Papua New Guinea. *Geochimica et Cosmochimica Acta*, **68**, 4405−4427.

Li, G., Peacor, D.R. and Coombs, D.S. (1997) Transformation of smectite to illite in bentonite and associated sediments from Kaka Point, New Zealand: Contrast in rate and mechanism. *Clays and Clay Minerals*, **45**, 54−67.

Marumo, K. and Hattori, K.H. (1999) Seafloor hydrothermal clay alteration at Jade in the back-arc Okinawa Trough: Mineralogy, geochemistry and isotope characteristics. *Geochimica et Cosmochimica Acta*, **63**, 2785−2804.

Masuda, H., O'Neil, J.R., Jiang, W.T. and Peacor, D.R. (1996) Relation between interlayer composition of authigenic smectite, mineral assemblages, I/S reaction rate and fluid composition in silicic ash of the Nankai Trough. *Clays and Clay Minerals*, **44**, 443−459.

Moss, R. and Scott, S.D. (2001) Geochemistry and mineralogy of gold-rich hydrothermal precipitates from the eastern Manus Basin, Papua New Guinea. *The Canadian Mineralogist*, **39**, 957−978.

Paulick, H., Vanko, D.A. and Yeats, C.J. (2004) Drill core-based facies reconstruction of a deep-marine felsic volcano hosting an active hydrothermal system (Pual Ridge, Papua New Guinea, ODP Leg 193). *Journal of Volcanology and Geothermal Research*, **130**, 31−50.

Peacor, D.R. (1992) Diagenetic and low-metamorphism of shales and slates. Pp. 335−380 in: *Minerals and Reactions at the Atomic Scale: Transmission Electron Microscopy* (P.R. Buseck, editor). Reviews in Mineralogy, **27**, Mineralogical Society of America, Washington D.C.

Peacock, M.A. (1926) The petrology of Iceland. Part I. The basic tuffs. *Transactions of the Royal Society of Edinburgh*, **55**, 53−76.

Post, J.E. and Burnham, C.W. (1986) Ionic modeling of mineral structures and energies in the electron gas approximation: TiO_2 polymorphs, quartz, forsterite, diopside. *American Mineralogist*, **71**, 142−150.

Shau, Y.H. and Peacor, D.R. (1992) Phyllosilicates in hydrothermally altered basalts from DSDP Hole 504B, Leg 83 − A TEM and AEM study. *Contributions to Mineralogy and Petrology*, **112**, 119−133.

Steiner, A. (1968) Clay minerals in hydrothermally altered rocks at Wairakei, New Zealand. *Clays and Clay Minerals*, **16**, 193−213.

Stroncik, N.A. and Schmincke, H.U. (2001) Evolution of palagonite: Crystallization, chemical changes, and element budget. *Geochemistry Geophysics Geosystems*, **2**, 2000GC000102.

Tazaki, K., Fyfe, W.S. and Van der Gaast, S.J. (1989) Growth of clay minerals in natural and synthetic glasses. *Clays and Clay Minerals*, **37**, 348−354.

Tilley, D.B. and Eggleton, R.A. (2005) Titanite low-temperature alteration and Ti mobility. *Clays and Clay Minerals*, **53**, 100−107.

Tomita, K., Yamane, H. and Kawano, M. (1993) Synthesis of smectite from volcanic glass at low temperature. *Clays and Clay Minerals*, **41**, 655−661.

Ufer, K., Roth, G., Kleeberg, R., Stanjek, H., Dohrmann, R. and Bergmann, J. (2004) Description of X-ray powder pattern of turbostratically disordered layer structures with a Rietveld compatible approach. *Zeitschrift für Kristallographie*, **219**, 519−527.

Yau, Y.C., Peacor, D.R. and Essene, E.J. (1987) Authigenic anatase and titanite in shales from the Salton Sea geothermal field, California. *Neues Jahrbuch für Mineralogie Monatshefte*, 441−452.

Zhou, Z. and Fyfe, W.S. (1989) Palagonitization of basaltic glass from DSDP Site 335, Leg 37: Textures, chemical composition, and mechanism of formation. *American Mineralogist*, **74**, 1045−1053.

Zhou, Z., Fyfe, W.S., Tazaki, K. and Van der Gaast, S.J. (1992) Structural characteristics of palagonite from DSDP Site 335. *The Canadian Mineralogist*, **30**, 75−81.

Zhou, W., Peacor, D.R., Alt, J.C., Van der Voo, R. and Kao, L.S. (2001) TEM study of the alteration of interstitial glass in MORB by inorganic processes. *Chemical Geology*, **174**, 365−376.